C. 2

NACA

RESEARCH MEMORANDUM

for the

Bureau of Aeronautics, Department of the Navy

AN INVESTIGATION OF THE LOW-SPEED STABILITY AND CONTROL

CHARACTERISTICS OF A $\frac{1}{10}$ -SCALE MODEL OF THE

MCDONNELL XF3H-1 AIRPLANE

TED NO. NACA DE 344

By John W. Draper

Langley Aeronautical Laboratory
Langley Field, Va.

CLASSIFICATION

UNCLASSIFIED

NATIONAL ADVISORY COMMITTEE
FOR AERONAUTICS
WASHINGTON

OCT 11 1951

NATIONAL ADVISORY COMMITTEE FOR AERONAUTICS

RESEARCH MEMORANDUM

for the

Bureau of Aeronautics, Department of the Navy

AN INVESTIGATION OF THE LOW-SPEED STABILITY AND CONTROL

CHARACTERISTICS OF A $\frac{1}{10}$ - SCALE MODEL OF THE

MCDONNELL XF3H-1 AIRPLANE

TED NO. NACA DE 344

By John W. Draper

SUMMARY

At the request of the Bureau of Aeronautics, Navy Department, an investigation of the low-speed, power-off stability and control charac-teristics of a $\frac{1}{10}$ - scale model of the McDonnell XF3H-1 airplane has been made in the Langley free-flight tunnel. Flight tests of the model in the clean and in the slats-and-flaps-extended conditions were made over a lift-coefficient range from about 0.5 through the stall. Only low-altitude conditions were simulated and no attempt was made to determine the effect on the stability characteristics of freeing the controls. Static force tests were made to determine the static longitudinal and lateral stability derivatives and rotary force tests were made to determine the dynamic rolling derivatives. Calculations were also made to determine the damping of the lateral oscillation for correlation with the flight results.

The longitudinal stability characteristics of the model were satis-factory for all conditions except near the stall where a nosing-up tendency was encountered. The nosing-up tendency could be controlled by the elevator. The stall was gentle and was characterized by the model settling to the floor of the test section with only small rolling, yawing, or pitching motions and with lateral control being maintained at all times. The lateral stability characteristics were generally satisfactory for all conditions tested and the yawing and rolling motions appeared

to be well-damped. The lateral controls of the model were somewhat weak but were considered to be adequate.

Analysis of force test data and stability calculations indicate that the airplane will have somewhat better lateral stability and control characteristics than the model and a less severe pitching-up tendency at the stall. Stability calculations indicate, however, that the dynamic lateral stability of the airplane at altitude will be worse than that indicated in the model flight tests which covered only low-altitude conditions.

INTRODUCTION

An investigation to determine the low-speed, dynamic stability characteristics of a $\frac{1}{10}$-scale model of the McDonnell XF3H-1 airplane has been made in the Langley free-flight tunnel at the request of the Bureau of Aeronautics, Navy Department. The XF3H-1 airplane is a jet-propelled airplane having 45° sweptback wings and tail surfaces.

Flight tests of the model to determine the dynamic stability characteristics were made over a lift-coefficient range from about 0.5 to the stall. Only low-altitude conditions were simulated. Static force tests were made to determine the static longitudinal and lateral stability characteristics and rotary force tests were made to determine the dynamic rolling derivatives. The model was tested in the clean and in the flaps-and-slats-extended conditions. The model was also tested with only the slats extended in order to increase the maximum lift and thereby extend the linear range of the stability derivatives so that this condition might more closely represent the full-scale airplane in the clean condition. Comparison is made between low Reynolds number force test results from the free-flight tunnel and results of higher Reynolds number force tests conducted at the Guggenheim Aeronautical Laboratory, California Institute of Technology (GALCIT) in order to permit a more accurate interpretation of the free-flight-tunnel test results in terms of the full-scale airplane. Calculations were made to determine the damping of the lateral oscillation for the model and the airplane at sea level for correlation with the results of the model flight tests.

SYMBOLS

All force and moment measurements were obtained with respect to the stability axes. A sketch showing the positive directions of the forces, moments, and angles is given in figure 1.

W   weight, pounds

S   wing area, square feet

$\bar{c}$ mean aerodynamic chord (M.A.C.), feet

b   wing span, feet

V   velocity, feet per second

q   dynamic pressure, pounds per square foot

ρ mass density of air, slugs per cubic foot

W/S   wing loading, pounds per square foot

m   mass, slugs

μ relative density factor $(m/\rho Sb)$

α angle of attack of fuselage center line, degrees

ψ angle of yaw, radians

β angle of sideslip ($-\psi$ in force tests), radians

C_L lift coefficient (Lift/qS)

C_D drag coefficient (Drag/qS)

C_m pitching-moment coefficient (Pitching moment/$qS\bar{c}$)

C_n yawing-moment coefficient (Yawing moment/qSb)

C_l rolling-moment coefficient (Rolling moment/qSb)

C_Y lateral-force coefficient (Lateral force/qS)

i_t tail incidence with respect to fuselage center line (positive with leading edge up), degrees

δ_e elevator deflection, degrees

δ_a aileron deflection, degrees

$$C_{Y_\beta} = \frac{\partial C_Y}{\partial \beta} \text{ per radian}$$

$$C_{n_\beta} = \frac{\partial C_n}{\partial \beta} \text{ per radian}$$

$$C_{l_\beta} = \frac{\partial C_l}{\partial \beta} \text{ per radian}$$

$\dfrac{pb}{2V}$ rolling-angular-velocity factor

p rolling angular velocity, radians per second

$\dfrac{rb}{2V}$ yawing-angular-velocity factor

r yawing angular velocity, radians per second

$$C_{l_p} = \frac{\partial C_l}{\partial \frac{pb}{2V}}$$

$$C_{n_p} = \frac{\partial C_n}{\partial \frac{pb}{2V}}$$

$$C_{Y_p} = \frac{\partial C_Y}{\partial \frac{pb}{2V}}$$

$$C_{l_r} = \frac{\partial C_l}{\partial \frac{rb}{2V}}$$

$$C_{n_r} = \frac{\partial C_n}{\partial \frac{rb}{2V}}$$

$$C_{Y_r} = \frac{\partial C_Y}{\partial \frac{rb}{2V}}$$

k_X radius of gyration about longitudinal body axis, feet

k_Z radius of gyration about vertical body axis, feet

k_{XZ} product-of-inertia factor about body axis, feet^2

k_{X_O} radius of gyration about longitudinal principal axis, feet

k_{Z_O} radius of gyration about vertical principal axis, feet

γ flight-path angle, degrees

ϵ angle between body axis and principal axis, positive when
           reference axis is above principal axis at nose of airplane,
           degrees

η angle of principal longitudinal axis of airplane, positive
           when principal axis is above flight path, degrees $(\alpha - \epsilon)$

$T_{1/2}$ time required for lateral oscillation to damp to one-half
           amplitude, seconds

Subscripts:

l left

r right

APPARATUS AND MODEL

The investigation was made in the Langley free-flight tunnel which
is designed to test free-flying dynamic models. A complete description
of the tunnel and its operation is given in reference 1. The rotary
tests made to determine the rolling derivatives were made on the Langley
20-foot free-spinning-tunnel rotary balance described in reference 2.

A three-view drawing of the model is presented in figure 2, and a
photograph of the model in the clean condition is presented in figure 3.
The photograph shows two stall vanes on each wing, but only the outboard
vanes were used in the investigation. Table I gives the scaled-up
dimensional and mass characteristics of the model.

The wing of the model had an NACA 0009-64 airfoil section which was
the same as that used on the full-scale airplane. The model had a 45°
sweptback wing with an aspect ratio of 3 and a taper ratio of 0.5. Stall
control vanes (P_{11}) located 0.84b/2 out on the wing panel (fig. 2) were
used for all free-flight-tunnel tests but the GALCIT model used for

comparison was equipped with combinations of the P_{11}, P_{30}, and P_3 stall vanes. The spanwise locations of these vanes are indicated in table I and the shapes are shown in reference 3. For all practical purposes, the P_{30} and P_{11} vane configurations are identical and should produce comparable results. (See table I.) The inlet ducts on the side of the fuselage were sealed and unfaired for all the free-flight-tunnel tests.

The aileron, spoiler, rudder, and elevator control surfaces were deflected by flicker-type mechanisms which gave either full-on or full-off control.

The ailerons and spoilers of the model could be used either independently or in combination for lateral control. The slats-extended configuration was obtained by replacing the removable leading edge of the wing with a leading edge incorporating a slat. The condition with flaps extended was obtained by replacing the wing trailing edge with a flapped trailing edge.

DETERMINATION OF STABILITY DERIVATIVES

OF FLIGHT-TEST MODEL

Force Tests

The static longitudinal and lateral stability and control characteristics of the model were determined from force tests made over an angle-of-attack range from $0°$ through the stall. The lateral characteristics were determined from measurements of force and moment coefficients at $\pm 5°$ yaw. All force tests were made at a dynamic pressure of 4.1 pounds per square foot which corresponds to an airspeed of approximately 40 miles per hour at standard sea-level conditions and to a test Reynolds number of 457,000 based on the mean aerodynamic chord of 1.22 feet. All forces and moments for the model are referred to a center of gravity located at 30 percent of the mean aerodynamic chord at a distance 24 percent of the mean aerodynamic chord above the bottom of the fuselage unless otherwise indicated.

The results of the free-flight-tunnel force tests are shown in figures 4 to 8. Also presented for comparison are higher scale data (Reynolds number of 2,180,000) obtained for a 0.15-scale model at GALCIT. These data were taken from reference 3. The GALCIT data are referred to a center-of-gravity position of 30 percent of the mean aerodynamic chord so that a direct comparison of the two sets of data was possible.

Longitudinal stability and control.- The results presented in figure 4 show that the lift-curve slopes of the two models in the clean condition were in good agreement at low lift coefficients but that the free-flight-tunnel model stalled at a much lower lift coefficient. From a comparison of pitching-moment curves it appears that the longitudinal stability characteristics of the two models were generally similar over the lift-coefficient range. The slats were extended to increase the maximum lift of the free-flight-tunnel model to a value more nearly representative of the larger scale model in an effort to provide a closer correlation of the free-flight-tunnel-model results with those for the full-scale airplane. With the slats extended the maximum lift coefficient was increased over that of the GALCIT model in the clean condition and the longitudinal stability compared fairly well in the lower lift-coefficient range. With the slats extended, however, there was a rather severe unstable break in the pitching-moment curve prior to the stall.

A comparison of the longitudinal stability characteristics of the two models with slats and flaps extended are shown in figure 5. Since GALCIT longitudinal data for the slats-and-flaps-extended condition with the final stall-vane configuration (P_{11}) were not available for comparison with the free-flight-tunnel data, GALCIT data for the P_3P_{11}-vane configuration are presented. Results of some preliminary tests of the free-flight-tunnel model with the P_3P_{11}- and P_{11}-vane configurations showed, however, that these two configurations had pitching-moment curves of about the same shape. The data presented in figure 5 show that in the slats-and-flaps-extended condition the two models had the same lift-curve slope and static longitudinal stability over most of the lift-coefficient range but the free-flight-tunnel model had a lower maximum lift coefficient and an earlier and sharper unstable break in the pitching-moment curve near the stall.

Lateral stability and control.- The data presented in figure 6 show that the derivatives C_{l_β}, C_{n_β}, and C_{Y_β} for the free-flight-tunnel model in the clean condition are in fairly good agreement with the GALCIT results except for the earlier break in the curves for the free-flight-tunnel model caused by the lower maximum lift coefficient. When the maximum lift coefficient was increased by extending the slats, the values of C_{n_β} were increased and were in better agreement with the values obtained for the GALCIT model. For C_{l_β}, however, extending the slats gave better agreement with the GALCIT value of C_{l_β} only up to the break in the GALCIT curve and beyond this point C_{l_β} increased to very large values. The data for the slats-and-flaps-extended condition (fig. 7) show excellent agreement between the lateral derivatives of the two models except for the earlier break in the free-flight-tunnel model data caused by the lower maximum lift coefficient.

The characteristics of the ailerons and spoilers determined from force tests are presented in figures 8(a) and 8(b) for the clean and the slats-and-flaps-extended conditions, respectively. A comparison with GALCIT data shows that the rolling moments were generally lower for the free-flight tunnel model but that the two models had about the same adverse yawing moments for all control configurations. Part of the loss of rolling moment on the free-flight-tunnel model can probably be attributed to the large leading-edge aileron gap which was not scaled from the airplane. In the clean configuration the difference in rolling moments between the two models decreased as the angle of attack increased; whereas in the slats-and-flaps-extended configuration the difference increased at the higher lift coefficients. The spoilers of both models when used with the ailerons produced only small additional rolling moments and had a slight effect on the yawing-moment characteristics.

Rotary Tests

The results of rotary tests made to determine the rolling derivatives C_{Y_p}, C_{n_p}, and C_{l_p} for the free-flight-tunnel model in the slats extended and the slats-and-flaps-extended configurations through an angle-of-attack range of $0°$ to $25°$ are presented in figure 9. The rotary tests were made at a dynamic pressure of 5.5 pounds per square foot which corresponds to a test Reynolds number of approximately 531,000 based on a mean aerodynamic chord of 1.22 feet.

The results of figure 9 show that the damping in roll C_{l_p} was approximately constant up to an angle of attack of about $15°$ for both configurations. Above an angle of attack of $15°$ the damping for the slats-and-flaps-extended condition decreased rapidly until the model became unstable. The decrease in damping for the slats-extended condition was more gradual but the model still became slightly unstable at the maximum lift coefficient. The yawing-moment-due-to-rolling parameter C_{n_p} was generally adverse and approximately of the same magnitude for both conditions up to about an angle of attack of $15°$. Above this angle of attack the yawing moment became more adverse for the model in the slats-and-flaps-extended condition but slightly favorable for the slats-extended condition.

FLIGHT TESTS

Flight tests of the model were made over a lift-coefficient range from about 0.5 through the stall for both the clean and slats-extended conditions. The center of gravity was located at 0.22 mean aerodynamic

chord for the model tests of the clean condition and varied between 0.20 and 0.27 mean aerodynamic chord for the slats-extended condition. The flight tests with the slats and flaps extended were made over a lift-coefficient range from about 0.7 through the stall with center-of-gravity locations from 0.21 to 0.30 mean aerodynamic chord. In general, flight tests to determine the longitudinal stability characteristics of the model were made over the center-of-gravity ranges indicated; whereas the lateral stability characteristics were determined with the center of gravity located in the most forward position. In all cases the wing loading was somewhat less than the scaled-down airplane values in order to minimize damage to the model in crashes.

Lateral control was obtained during the flight tests by deflecting the ailerons alone or in conjunction with the spoilers which were extended full up with the upward-deflected aileron. The characteristics of these controls were studied with and without coordinated rudder control.

CALCULATIONS

Calculations to determine the period and the time to damp to one-half amplitude of the lateral oscillation of both the model and the airplane were made by the method of reference 4. Results were obtained for the model in the slats-extended and in the slats-and-flaps-extended conditions and for the airplane in the clean and slats-and-flaps-extended conditions.

The aerodynamic and mass characteristics used in the calculations are presented in table II. The values of C_L, C_{n_β}, C_{l_β}, and C_{Y_β} for the model were obtained from force tests, and the values for the airplane were obtained from reference 3. The values of C_{Y_r}, C_{n_r}, and C_{l_r} for the model and the airplane were estimated from references 5 to 7. The values of C_{Y_p}, C_{n_p}, and C_{l_p} for both the model and airplane were obtained from the data of figure 9.

RESULTS AND DISCUSSION

Interpretation of Flight-Test Results

In interpreting the results of the model flight tests in terms of the full-scale airplane it is necessary to consider the differences between the aerodynamic and scaled-up mass characteristics of the model and those of the airplane. If these aerodynamic and mass characteristics

are the same for the airplane as those of the model, the airplane would
be expected to exhibit dynamic characteristics similar to those of the
free-flight-tunnel model.

It can be seen from table I that the scaled-up weight of the model
is less than the weight of the airplane but that the moments of inertia
of the scaled-up model are somewhat higher than those of the airplane.
The net result of these two effects will probably be to make the model
results conservative from the standpoint of dynamic lateral stability.

In this investigation it has been shown that the static stability
characteristics of the low-scale, free-flight-tunnel model are in fairly
good agreement with the results of the higher-scale tests if it is
considered that the maximum lift coefficient of the model is less than
that of the airplane, and, therefore, that the variation of the model
derivatives with lift coefficient will depart from linearity at lower
lift coefficients than those of the airplane. The dynamic stability
characteristics of the model in the clean condition should, because of
its aerodynamic similarity to the higher-scale model, be fairly represent-
ative of the dynamic longitudinal and lateral stability of the airplane.
As has been pointed out previously, by extending the slat it was possible
to increase the lift range over which the model would represent the
lateral stability characteristics of the airplane in the clean condition.
Although the values of C_{l_β} for the slats-extended condition were greater
than those for the larger-scale GALCIT model in the clean condition, the
slats-extended condition was thought to be of interest to flight test
since it might be considered to represent the maximum values of C_{l_β}

that the airplane could have in the clean condition. The longitudinal
and lateral stability characteristics of the model with slats and flaps
extended should be fairly representative of the airplane in that condi-
tion except for greater longitudinal instability near the stall and the
loss in maximum lift caused by the low scale of the tests.

It should be pointed out that the full-scale airplane should be
easier to fly than the model because its angular velocities are about
one-third as fast as those of the model. The lateral control of the
airplane should also be better because the model rolling inertia was
higher and the aileron effectiveness was lower than those expected for
the airplane.

Clean Condition

The longitudinal stability of the model in the clean condition was
satisfactory up to a lift coefficient of about 0.6 with the center of
gravity located at approximately 0.22 mean aerodynamic chord. At higher
lift coefficients the model appeared to have about neutral longitudinal

stability and developed a slight pitching-up tendency prior to the stall although the pitching-moment curve for a center-of-gravity position of 0.22 mean aerodynamic chord (fig. 10) indicates that the model did not actually become unstable. The stall was gentle and was characterized by the model settling to the floor of the tunnel with only small rolling or yawing motions and with lateral control being maintained at all times. This longitudinal instability experienced near the stall appeared to be somewhat worse for the present model than that experienced by the McDonnell XF-88 model with stall control vanes (reference 8), although the degree of static stability as shown by the pitching-moment curves was about the same for both models. Although flights were not made with a center-of-gravity position rearward of 0.22 mean aerodynamic chord a rearward shift of the center of gravity to 0.30 mean aerodynamic chord would increase the instability of the model at high lift coefficients. It is expected that the resulting pitching motion would be considered objectionable by the pilot but, on the basis of the slats-extended flight tests, which are discussed in a later section, it would probably still be controllable by the elevator.

Flight tests showed that the lateral stability characteristics of the model were satisfactory over the lift range tested. The decrease in static directional stability at the high lift coefficients (see fig. 6) did not appear to affect the flight characteristics. The yawing and rolling motions following a disturbance were well-damped.

The response of the model to lateral control was satisfactory but the controls were somewhat weaker than those of the McDonnell XF-88 model (reference 8). The control characteristics obtained from the model flight tests should be considered conservative, however, since the rolling moment produced by the ailerons is less than that of the higher-scale GALCIT model (fig. 8(a)) and the scaled-up rolling inertia of the free-flight-tunnel model is greated than that of the airplane. Using the spoiler in conjunction with the aileron had no appreciable effect on the control characteristics.

Slats-Extended Condition

The longitudinal and lateral stability and control characteristics as well as the behavior at the stall with slats extended were generally the same as those for the clean condition when the model was flown with center-of-gravity locations as far rearward as 0.27 mean aerodynamic chord. The pitching-up motion associated with the break in the pitching-moment curve (fig. 10) was more severe than that exhibited in the clean condition with comparable center-of-gravity locations, but the motion could still be controlled with the elevator. This unstable condition did not extend through the stall and the model could be trimmed to fly at lift coefficients just below the stall where the pitching-moment

curve was again stable. Although the maximum rearward position of the
center of gravity investigated during flight tests was 0.27 mean aero-
dynamic chord, it appears from figure 4 that the break in the pitching-
moment curve for the free-flight model with slats extended with the
center of gravity at this position would still be worse than that for
the higher-scale model in the clean condition with the center of gravity
located as far rearward as 0.30 mean aerodynamic chord. Thus the model
results should be conservative when used as a basis for evaluating the
flight behavior of the airplane.

The large increase in C_{l_β} caused by extending the slats had
surprisingly little effect on the flying characteristics of the model.
Although the model in the clean condition had values as low as might be
expected of the airplane and the model in the slats-extended condition
had values of C_{l_β} as high as might be expected of the airplane, no
appreciable effects of these large changes in C_{l_β} were noted on the
dynamic lateral stability characteristics of the model. It appears,
therefore, that an accurate estimation of C_{l_β} is not necessary for
evaluating the lateral stability characteristics of the airplane in the
clean condition.

Calculated values of the damping of the lateral oscillation (fig. 11)
for the model in the slats-extended condition are in qualitative agree-
ment with the flight tests in that they show satisfactory damping of
the oscillatory mode. A comparison of the calculated damping character-
istics for the model as flown with slats extended and for the airplane
in the clean condition at sea level indicate that the model flight
results are probably slightly conservative. Also presented in figure 11
are the results of calculation for the airplane which were taken from
reference 9 and show the effects of altitude on the damping. Although
these calculations are not directly comparable with the calculations of
the present investigation, they are of interest since they show the
effect of increasing altitude on the damping characteristics. These
results show that the dynamic lateral stability at altitude would be
worse than that noted in the model flight tests which covered only low-
altitude conditions.

Slats-and-Flaps-Extended Condition

Flights of the model in the slats-and-flaps-extended condition with
the center of gravity located between 0.21 and 0.30 mean aerodynamic
chord showed that the longitudinal stability characteristics of the
model were approximately the same as those for the clean condition, with
satisfactory stability through the lower lift range and a pitching-up
tendency at the higher lift coefficients. The pitching-up tendency

became more severe as the center of gravity was moved rearward from 0.21 to 0.30 mean aerodynamic chord, but the motion could still be controlled by the elevator. At the stall there was little apparent difference in the behavior of the model in the slats-and-flaps-extended condition when compared with the behavior of the model in the clean and slats-extended conditions. The stall was still considered to be mild but the rolling and yawing motions were slightly greater than in the clean condition. The stall was characterized by the model settling to the floor of the tunnel with lateral control being maintained at all times.

Flight tests showed that the lateral stability characteristics were satisfactory over the lift range tested even though the calculations (fig. 11) indicated unsatisfactory damping of the lateral oscillation of the model. The calculations also show a marked difference in the damping between the slats-extended condition and the slats-and-flaps-extended conditions which was not shown by the model flight tests. The reason for the discrepancies between the flight tests and calculations is not known.

The lateral control characteristics were considered to be about the same as for the clean condition. The control was adequate but was weaker than that of the McDonnell XF-88 model in the flaps-down condition (reference 8). As previously pointed out the control characteristics as determined from the model tests are considered to be conservative because of the lower aileron effectiveness and higher inertia of the model.

CONCLUSIONS

The following conclusions were drawn from the results of the free-flight-tunnel stability and control investigation of a $\frac{1}{10}$-scale model of the McDonnell XF3H-1 airplane. Flight tests were made over a lift-coefficient range from about 0.5 through the stall. Only low-altitude conditions were simulated and no attempt was made to determine the effect on the stability characteristics of freeing the controls.

1. The longitudinal stability characteristics of the model were satisfactory for all conditions except near the stall where a nosing-up tendency was encountered. The nosing-up tendency could be controlled with the elevator.

2. The lateral stability characteristics were generally satisfactory for all conditions and the yawing and rolling motions were well-damped. Lateral control was considered to be adequate.

NACA RM SL51J12

3. The stall was gentle for all conditions and was characterized by the model settling to the floor with only small pitching, rolling, and yawing motions and with lateral control being maintained at all times.

4. Analysis of force test data and stability calculations indicate that the airplane will have somewhat better lateral stability and control characteristics than the model and a less severe pitching-up tendency at the stall. Stability calculations indicate, however, that the dynamic lateral stability of the airplane at altitude will be worse than that indicated in the model flight tests which covered only low-altitude conditions.

Langley Aeronautical Laboratory
    National Advisory Committee for Aeronautics
        Langley Field, Va.

John W. Draper
Aeronautical Research Scientist

Approved: Charles H. Zimmerman
      for   Thomas A. Harris
    Chief of Stability Research Division

ecc

REFERENCES

1. Shortal, Joseph A., and Osterhout, Clayton J.: Preliminary Stability and Control Tests in the NACA Free-Flight Wind Tunnel and Correlation with Full-Scale Flight Tests. NACA TN 810, 1941.

2. Stone, Ralph W., Jr., Burk, Sanger M., Jr., and Bihrle, William, Jr.: The Aerodynamic Forces and Moments of a $\frac{1}{10}$-Scale Model of a Fighter Airplane in Spinning Attitudes as Measured on a Rotary Balance in the Langley 20-Foot Free-Spinning Tunnel. NACA TN 2181, 1950.

3. Stephens, Robert: Model XF3H-1. Summary of 15% Scale Low Speed Wind Tunnel Model Data on Stability and Control. Rep. No. 1474, McDonnell Aircraft Corp., Dec. 7, 1949.

4. Sternfield, Leonard: Some Considerations of the Lateral Stability of High-Speed Aircraft. NACA TN 1282, 1947.

5. Letko, William, and Cowan, John W.: Effect of Taper Ratio on Low-Speed Static and Yawing Stability Derivatives of 45° Sweptback Wings with Aspect Ratio of 2.61, NACA TN 1671, 1948.

6. Campbell, John P., and Goodman, Alex: A Semiempirical Method for Estimating the Rolling Moment Due to Yawing of Airplanes. NACA TN 1984, 1949.

7. Campbell, John P., and McKinney, Marion O.: Summary of Methods for Calculating Dynamic Lateral Stability and Response and for Estimating Lateral Stability Derivatives. NACA TN 2409, 1951.

8. Schade, Robert O.: Investigation of Low-Speed, Power-Off Stability and Control Characteristics of a Model with a 35° Sweptback Wing in the Langley Free-Flight Tunnel. NACA RM L8A14, 1948.

9. Clark, D. D.: Model XF3H-1. Summary of Preliminary Lateral-Directional Dynamic Stability Calculations. Rep. No. 1544, McDonnell Aircraft Corp., Jan. 20, 1950.

10. Stamps, F. M.: Model XF3H-1. Estimated Moments of Inertia. Rep. No. 1139, McDonnell Aircraft Corp., April 29, 1949.

NACA RM SL51J12

TABLE 1.- DIMENSIONAL AND MASS CHARACTERISTICS OF THE MCDONNELL XF3H-1 AIRPLANE AND SCALED UP

CHARACTERISTICS OF THE $\frac{1}{10}$-SCALE MODEL TESTED IN THE LANGLEY FREE-FLIGHT TUNNEL

Characteristics	Scaled-up model values			Full scale	
	Configuration			Configuration	
	Clean	Clean with slats	Landing	Clean	Landing
Weight, lb	14,650	14,850	15,200	17,593	16,969
Relative density factor, $(m/\rho Sb)$	13.10	13.25	13.60	15.71	15.16
Moment of inertia:					
I_X, slug-ft^2	16,400	17,000	17,200	12,078	13,279
I_y, slug-ft^2	82,000	64,200	81,800	48,654	49,603
I_z, slug-ft^2	90,500	92,100	92,600	56,702	57,828
Wing loading, lbs/sq ft	35.3	35.8	36.6	42.5	41.0

Wing:
Airfoil section. . . . . NACA 0009-64
Area, sq ft 415
Span, ft 35.3
Sweepback, c/4, deg 45
Incidence, deg 2.07
Dihedral, deg (mean line) 0
Taper ratio 0.5
Aspect ratio 3.0
Mean aerodynamic chord, ft 12.2
Location of leading edge M.A.C. behind
  leading edge of root chord, ft 8.8
Root chord (parallel to chord line), ft 15.66
Tip chord (parallel to chord line), ft 7.83
Distance from nose to leading edge
  of root chord, ft 14.9

Aileron:
Area (one aileron), percent wing area 3.06
Span (one aileron), percent wing span 16.1
Hinge location, percent chord 0.78

Vertical tail:
Area (from top of fuselage), sq ft 57
Span (from top of fuselage), ft 7.12
Aspect ratio 0.89
Sweepback, c/4, deg 45
Taper ratio 0.50
Mean aerodynamic chord, ft 6.37
Tail length (from 30 percent M.A.C.$_{wing}$
  to 25 percent M.A.C.$_{tail}$), ft 22.8

Horizontal tail:
Area, sq ft 60
Span, ft 13.4
Aspect ratio 3.0
Sweepback, c/4, deg 45
Taper ratio 0.50
Mean aerodynamic chord, ft 4.61
Tail length (from 30 percent M.A.C.$_{wing}$
  to 25 percent M.A.C.$_{tail}$), ft 24.6

Leading-edge slat:
Chord, constant, ft 1.616
Span, percent of wing span 100

Trailing-edge flap (slotted):
Chord, percent of wing chord 20
Span, percent of wing span 19
Deflection, deg 40

[a]Spoilers:
Height, in. 8.30
Location, percent of wing chord 70
Span, percent of wing span 22.4

Stall vanes:
Height, in. 6.6
Location, percent of wing semispan
  P$_{11}$ 84.2
  P$_{30}$ (airplane only) 83.5
  P$_3$ (airplane only) 68

[a]Projected area reduced approximately 40 percent by perforations.

TABLE II.- AERODYNAMIC AND MASS CHARACTERISTICS USED IN CALCULATING THE DAMPING

AND PERIOD OF THE MODEL AND OF THE AIRPLANE

Characteristics	Model				Airplane (a)			
	Slats extended		Slats and flaps extended		Clean		Slats and flaps extended	
C_L	0.485	0.90	0.90	1.28	0.485	0.90	0.90	1.28
μ, slugs	13.25	13.25	13.60	13.60	15.71	15.71	15.16	15.16
$k_{X_0}^2/b$	.030	.030	.030	.030	.0175	.0175	.0200	.0200
$k_{Z_0}^2/b$	.165	.165	.161	.161	.0836	.0836	.0872	.0872
η	5.4	13.4	5.7	13.7	3.1	12.5	4.6	12.0
K_X^2	.0312	.0372	.0313	.0373	.0177	.0206	.0204	.0229
K_Z^2	.1638	.1578	.1597	.1536	.0834	.0805	.0868	.0843
K_{XZ}	.0126	.0304	.0129	.0301	.0036	.0140	.0054	.0137
C_{l_p}	-.350	-.360	-.400	-.300	-.340	-.360	-.400	-.200
C_{Y_β}, radians	-.745	-.630	-.688	-.630	-.688	-.688	-.802	-.688
C_{l_r}	.130	.150	.160	.180	.130	.150	.160	.180
C_{n_p}	-.030	-.010	-.035	-.050	-.030	-.010	-.035	-.050
C_{n_r}	-.290	-.310	-.310	-.350	-.290	-.310	-.310	-.350
C_{Y_p}	.060	.100	.195	.200	.060	.100	.195	.200
C_{Y_r}	-.400	-.400	-.400	-.400	-.400	-.400	-.400	-.400
C_{n_β}, radians	.192	.155	.200	.172	.189	.166	.195	.178
C_{l_β}, radians	-.103	-.172	-.246	-.298	-.109	-.143	-.240	-.275
$\tan \gamma$	-.176	-.287	-.249	-.249	-.176	-.287	-.249	-.249

[a]Mass data obtained from reference 10.
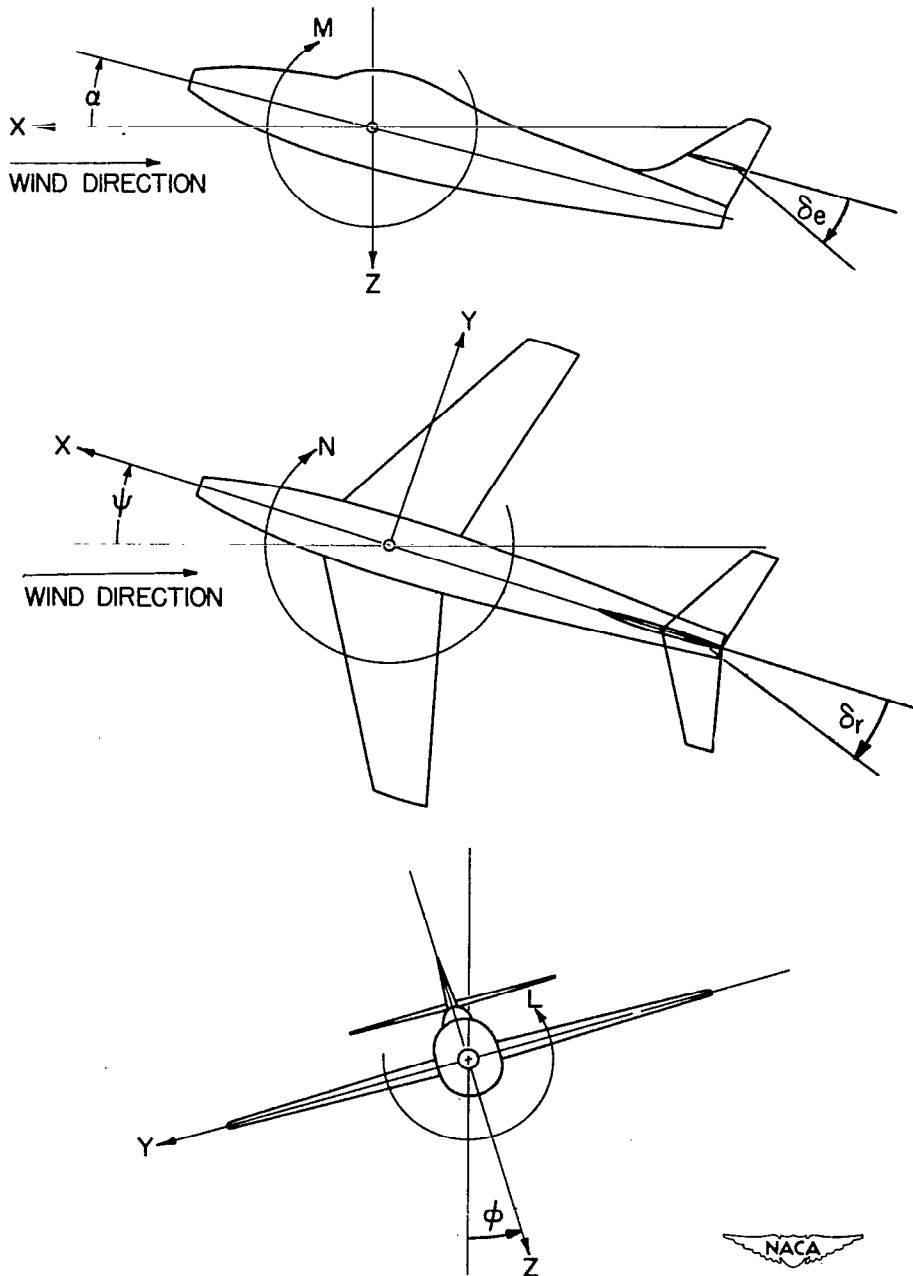
Figure 1.- The stability system of axes. Arrows indicate positive
   directions of moments, forces, and control-surface deflections.
   This system of axes is defined as an orthogonal system having
   the origin at the center of gravity and in which the Z-axis is
   in the plane of symmetry and perpendicular to the relative wind,
   the X-axis is in the plane of symmetry and perpendicular to the
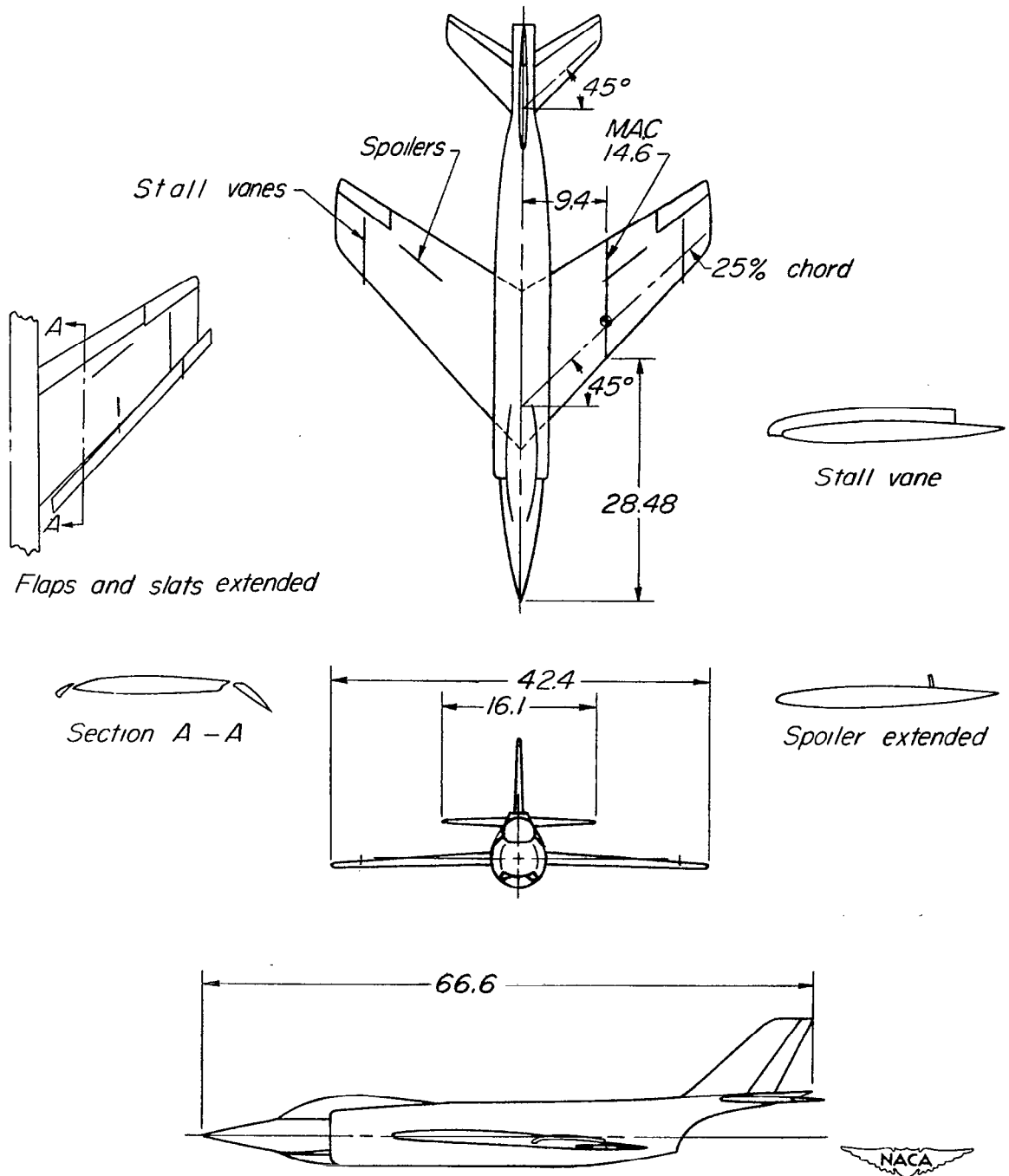   Z-axis, and the Y-axis is perpendicular to the plane of symmetry.

Figure 2.- Three-view drawing of $\frac{1}{10}$ - scale model of the XF3H-1 airplane. All dimensions are in inches.
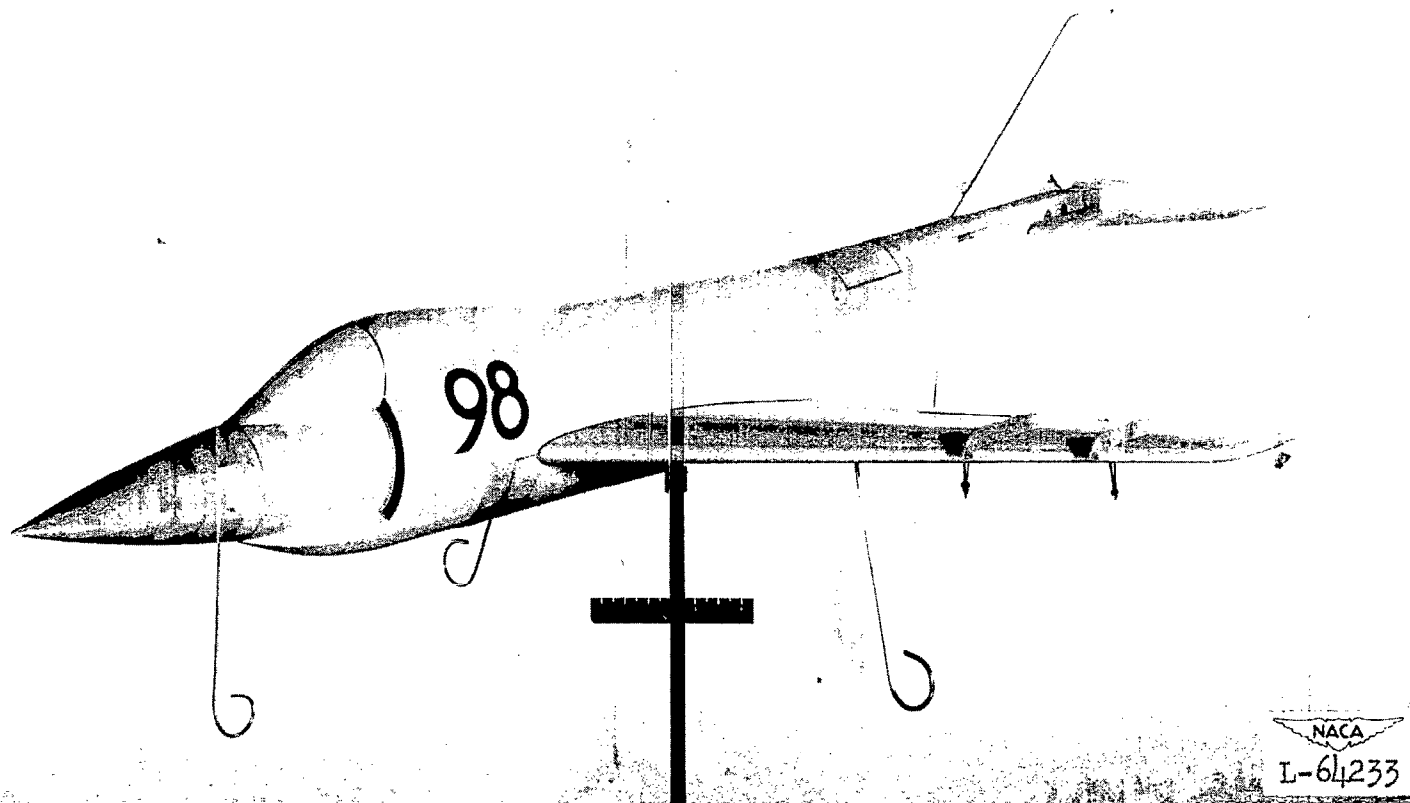
Figure 3.- Three-quarter front view of $\frac{1}{10}$-scale model of the XF3H-1 model, clean condition. (Only outboard stall vanes were used in the tests.)
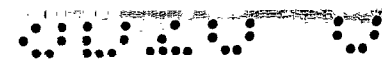
L-64233
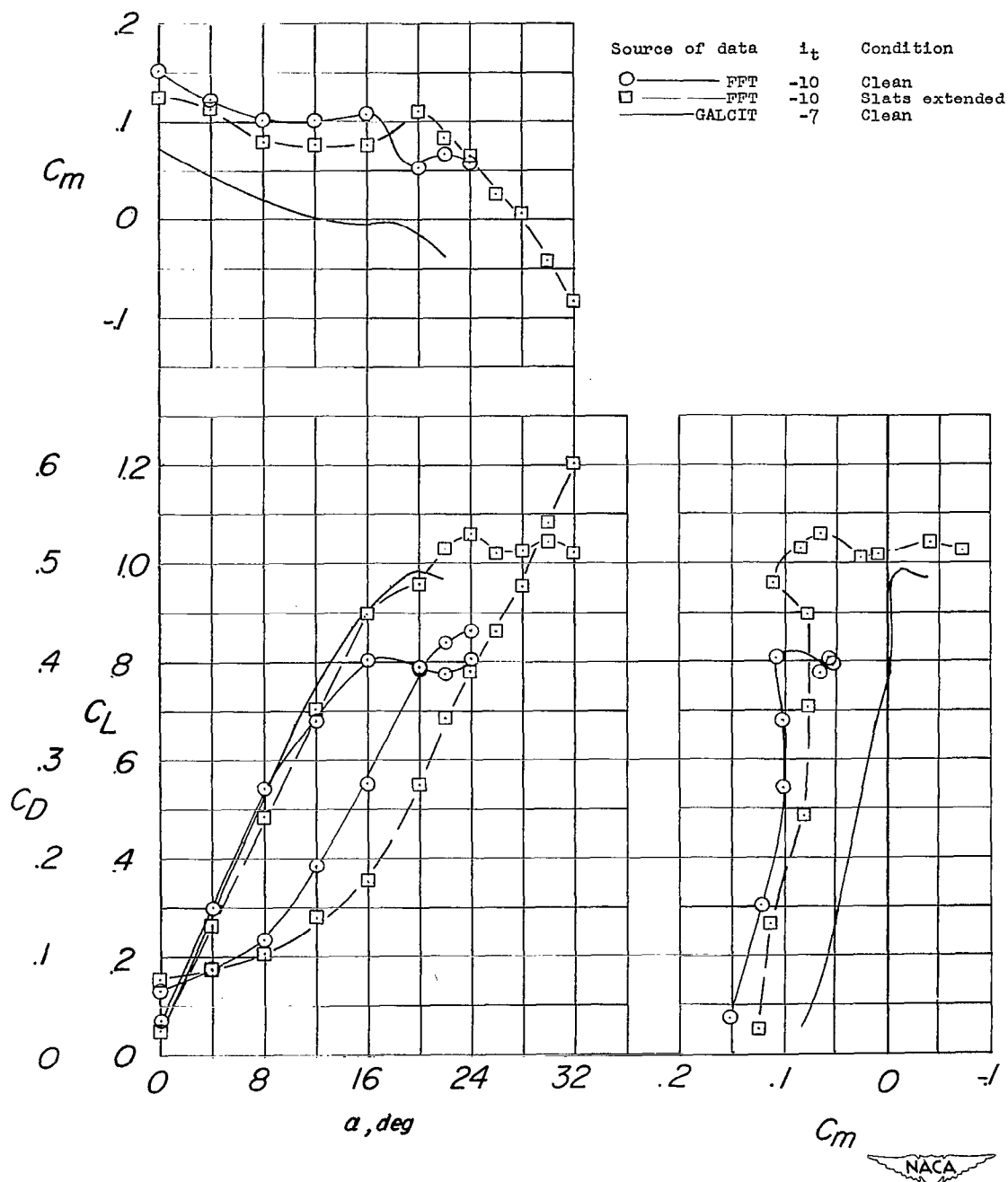
Figure 4.- Comparison of the longitudinal stability characteristics of the free-flight-tunnel and GALCIT models in the clean condition and the free-flight-tunnel model in the slats extended condition. All conditions with $\delta_e = 0^\circ$, flaps retracted and with P_{11}-stall-vane configuration.

Figure 5.- Comparison of the longitudinal stability characteristics of the free-flight-tunnel model and GALCIT model in the flaps-and-slats-extended condition with $\delta_e = 0°$.
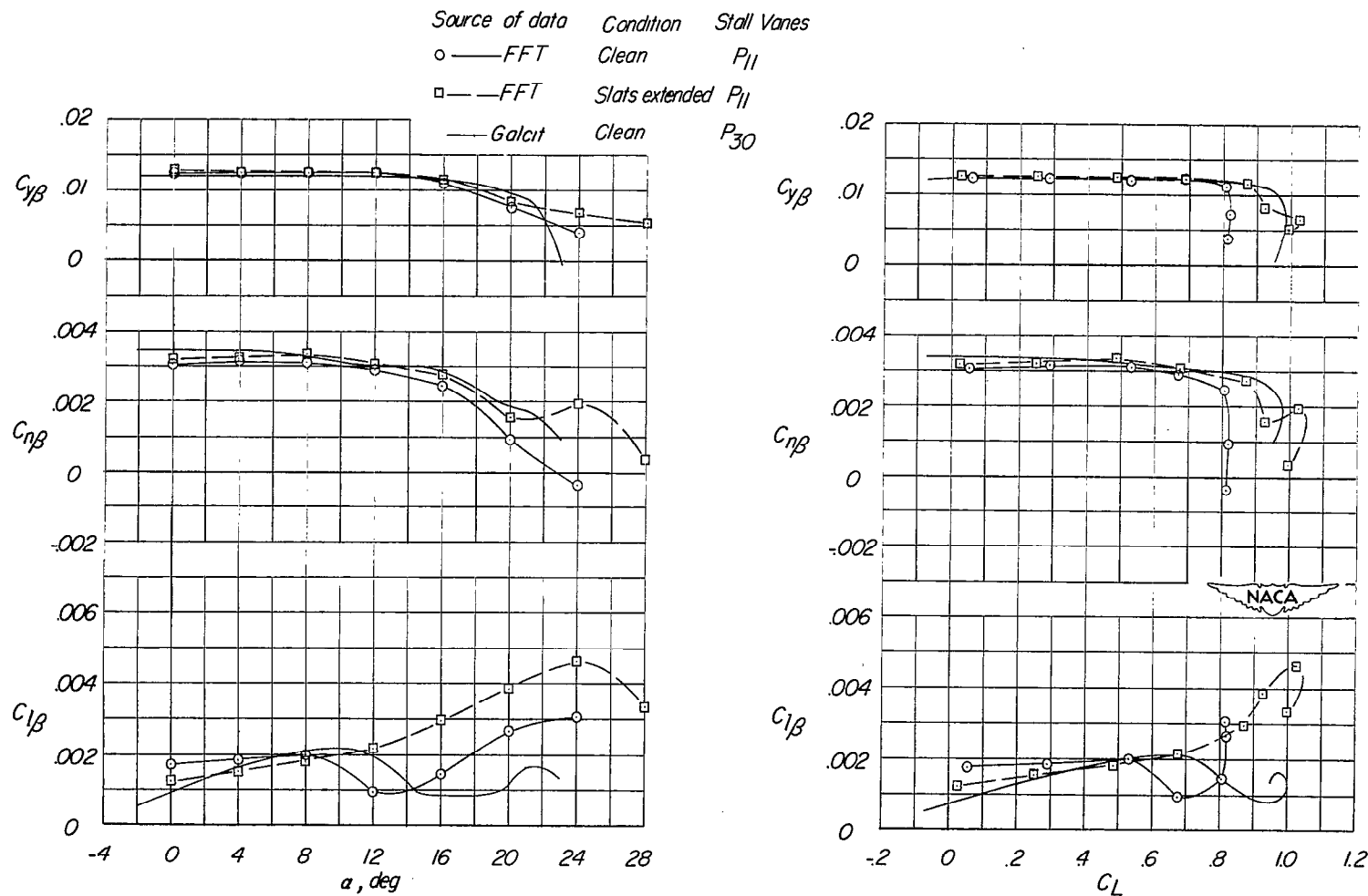
Figure 6.- Lateral stability characteristics of the free-flight-tunnel
model and GALCIT model in the clean condition and the free-flight-
tunnel model in the slats-extended condition. The values of i_t
and δ_e are unknown for the GALCIT data and for the free-flight-
tunnel tests are -10 and -8, respectively. Flaps were retracted
for all tests.
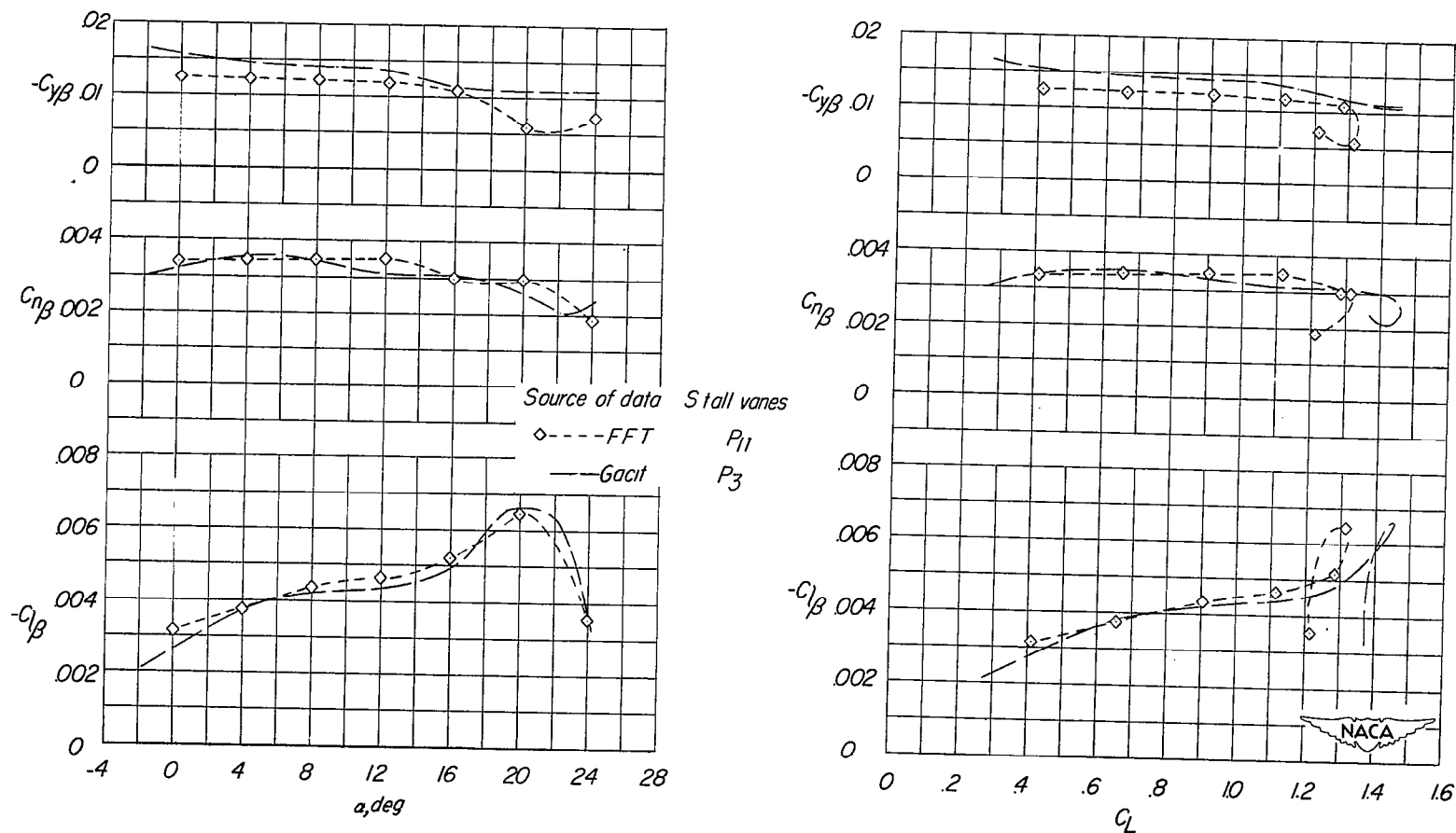
Figure 7.- Lateral stability characteristics of the free-flight-tunnel model and GALCIT model with slats and flaps extended. The values of i_t and δ_e are unknown for the GALCIT data and for the free-flight-tunnel tests are -10 and -8, respectively.

Source of data	Condition	Right spoiler
FFT	Clean	Extended
FFT	Slats extended	Extended
FFT	Slats extended	Retracted
GALCIT	Clean	Extended
GALCIT	Clean	Retracted
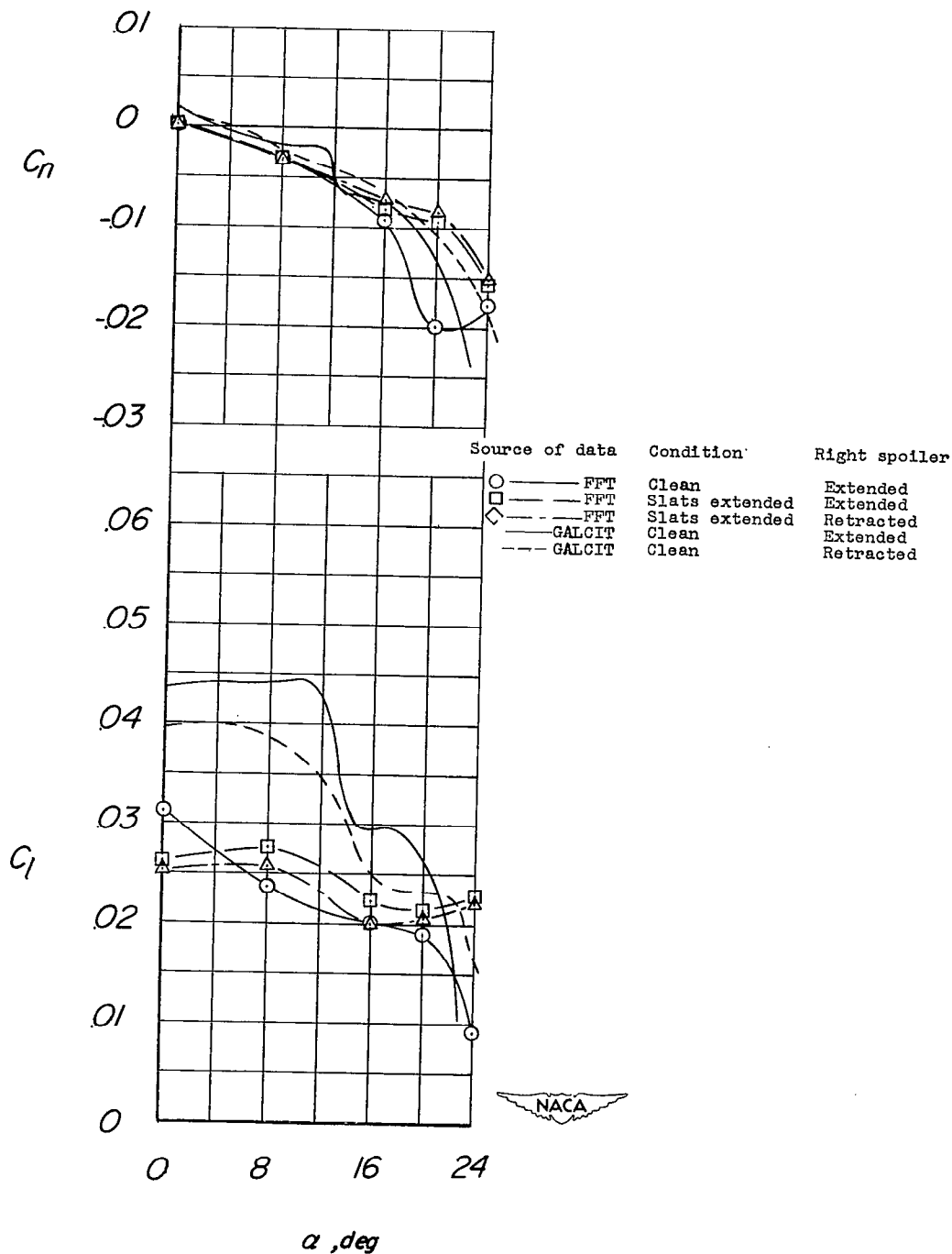
(a) Clean and slats-extended conditions.

Figure 8.- Rolling and yawing characteristics of ailerons and spoilers of the free-flight-tunnel model and GALCIT models. $\delta_{a_r} = -30°$; $\delta_{a_l} = 30°$; left spoiler retracted for all tests.
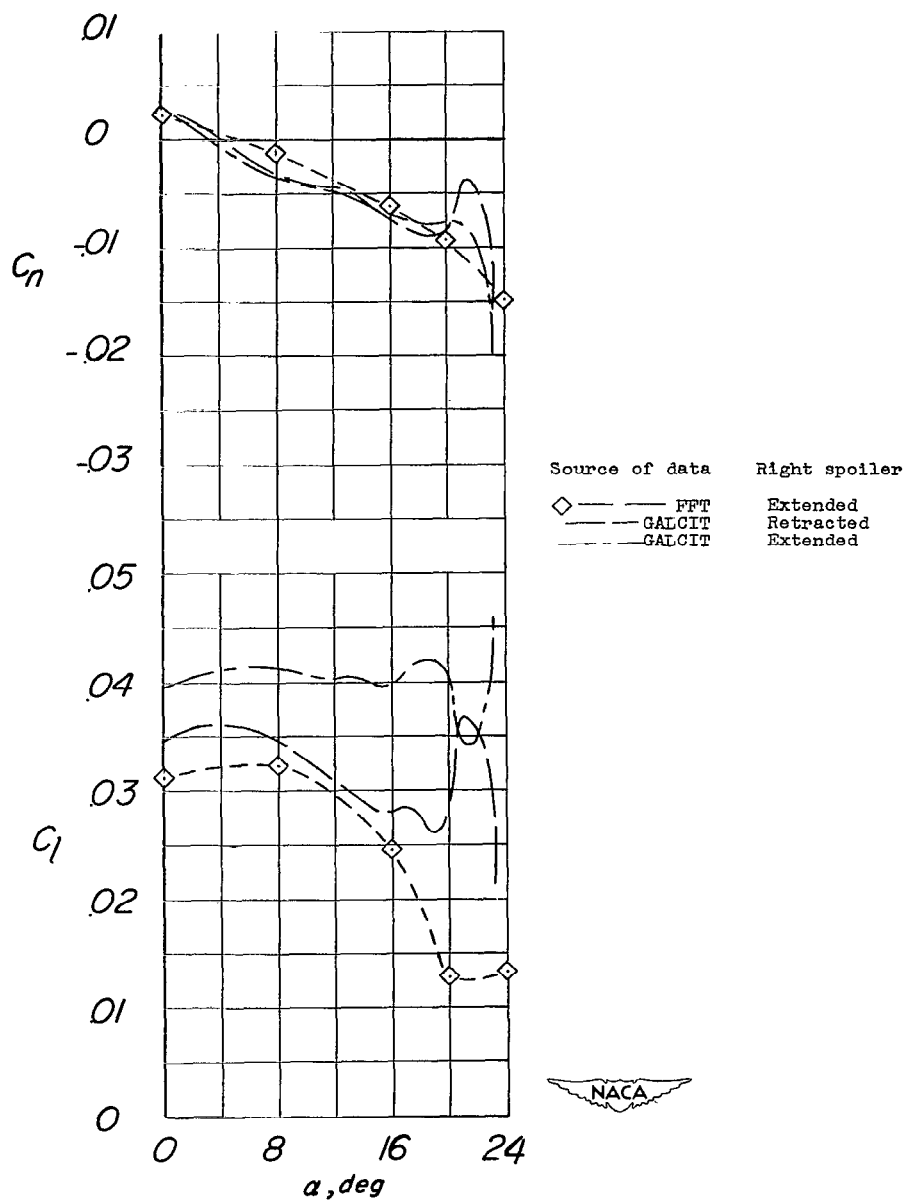
(b) Flaps and slats extended.

Figure 8.- Concluded.
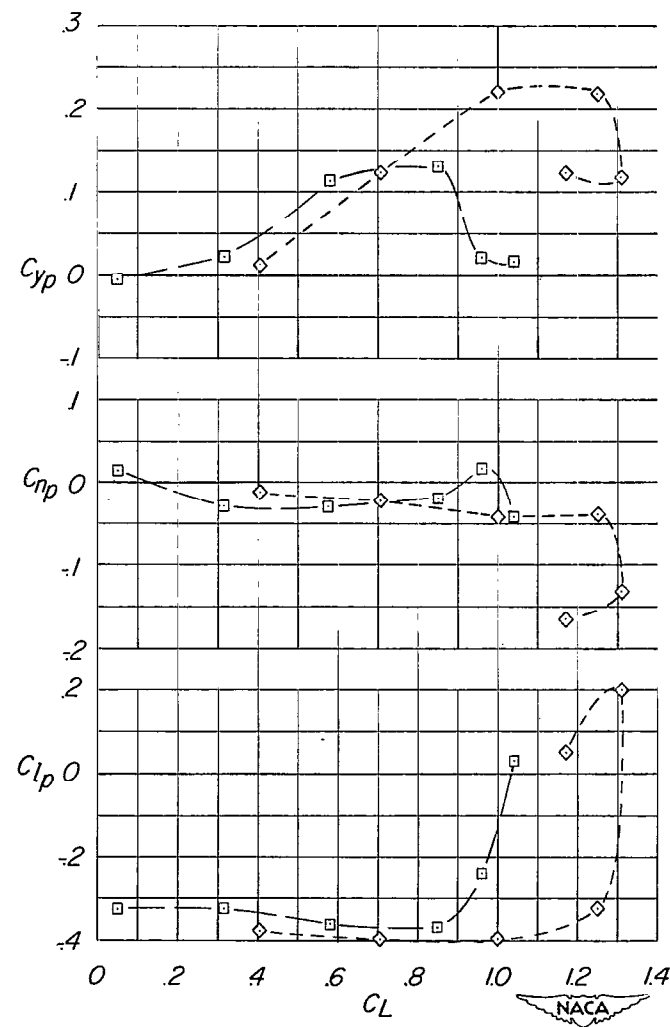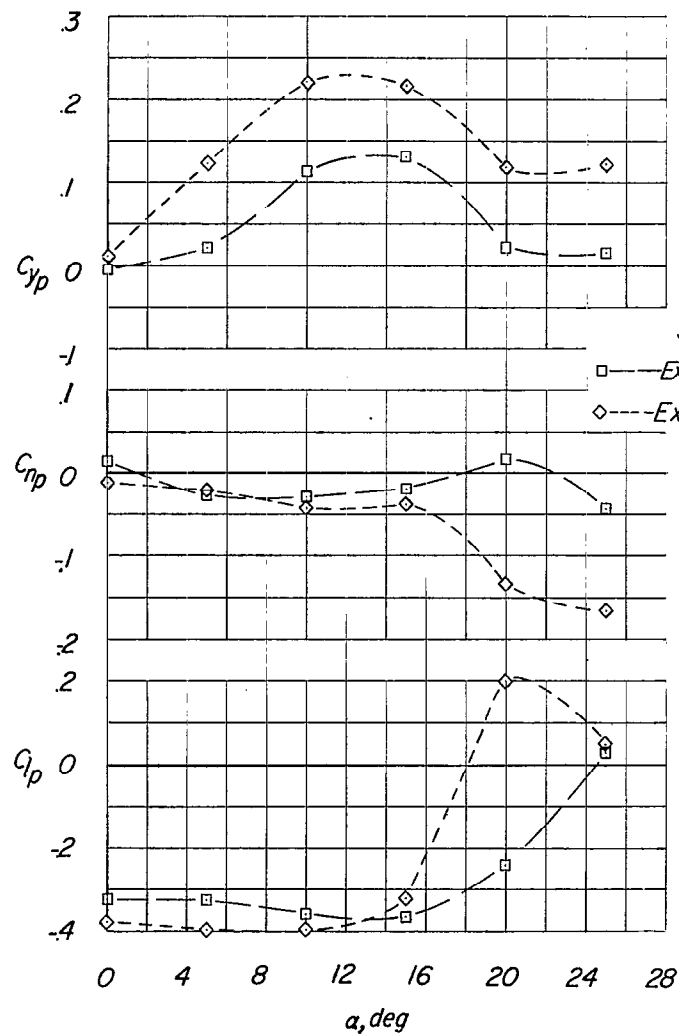
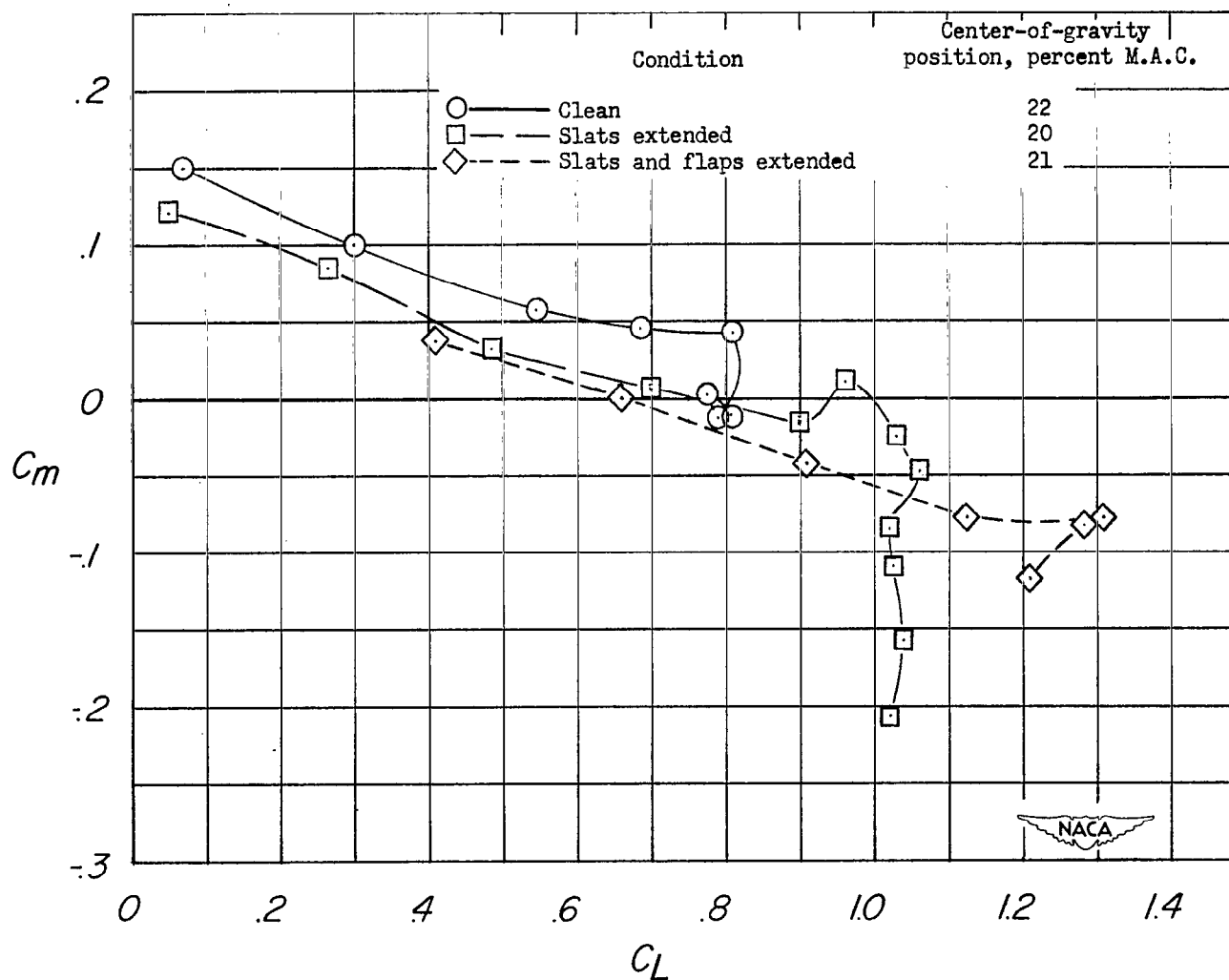Figure 9.- Rolling derivatives obtained on the free-flight-tunnel model.

Figure 10.- Pitching characteristics of the free-flight-tunnel model
of the XF3H-1 airplane with the most forward center-of-gravity
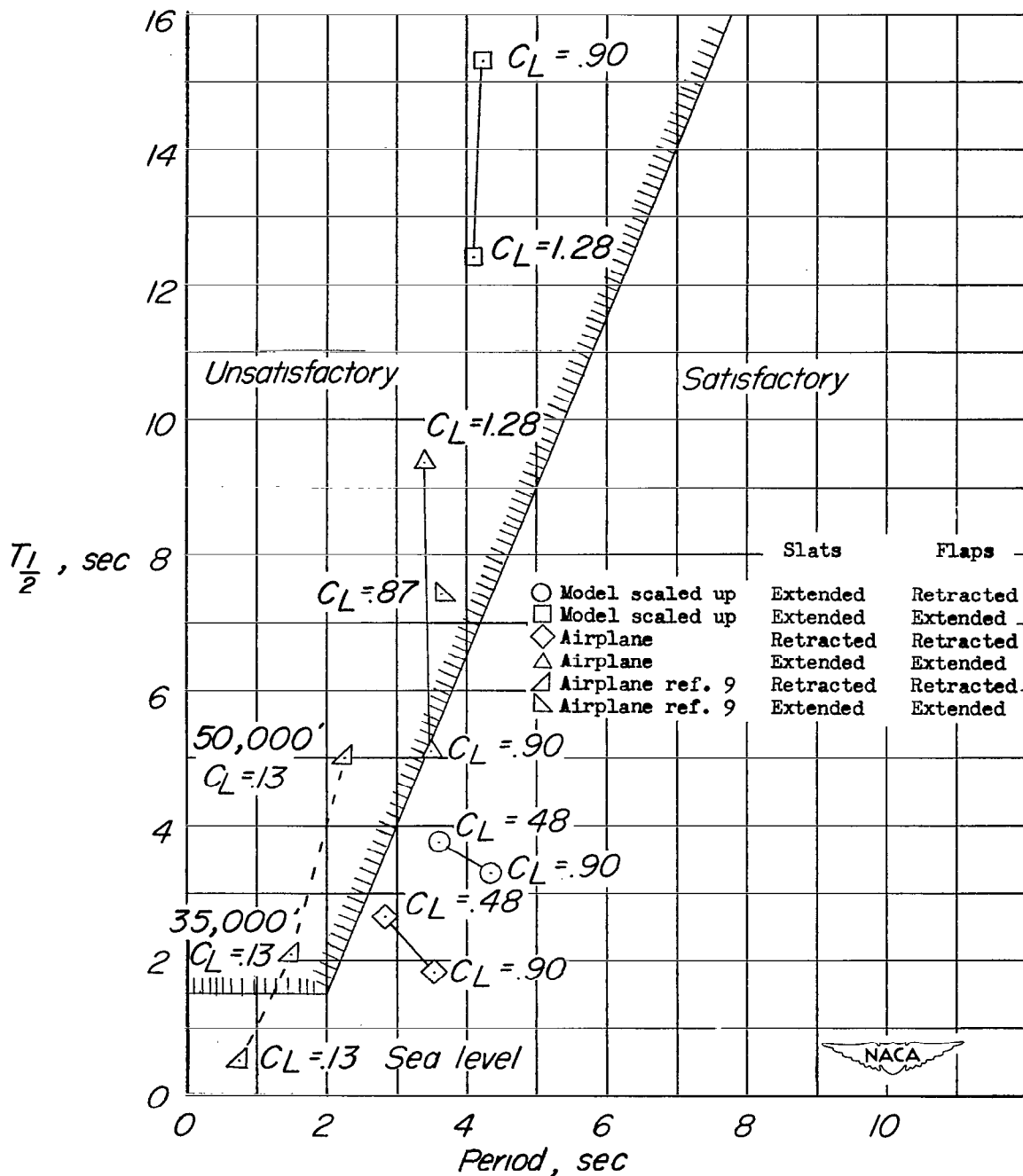positions in which the model was flight tested. $\delta_e = 0^o$.

Figure 11.- Comparison of the calculated damping and period characteristics of the McDonnell XF3H-1 airplane with the U. S. Air Force and Navy flying-qualities specifications.